Concepts of nuclear α-particle condensation

Y. Funaki,[1] H. Horiuchi,[2,3] W. von Oertzen,[4,5] G. Röpke,[6] P. Schuck,[7,8,9] A. Tohsaki,[2] and T. Yamada[10]

[1]*Institute of Physics, University of Tsukuba, Tsukuba 305-8571, Japan*
[2]*Research Center for Nuclear Physics, Osaka University, Osaka 567-0047, Japan*
[3]*International Institute for Advanced Studies, Kizugawa 619-0225, Japan*
[4]*Hahn-Meitner-Institut Berlin, Glienicker Strasse 100, D-14109 Berlin, Germany*
[5]*Freie Universität Berlin, Fachbereich Physik, Arnimallee 14, D-14195 Berlin, Germany*
[6]*Institut für Physik, Universität Rostock, D-18051 Rostock, Germany*
[7]*Institut de Physique Nucléaire, F-91406 Orsay CEDEX, France*
[8]*Université Paris-Sud, F-91406 Orsay CEDEX, France*
[9]*Laboratoire de Physique et Modélisation des Milieux Condensés, CNRS et Université Joseph Fourier, 25 Avenue des Martyrs, BP 166, F-38042 Grenoble CEDEX 9, France*
[10]*Laboratory of Physics, Kanto Gakuin University, Yokohama 236-8501, Japan*

(Received 7 February 2009; revised manuscript received 1 October 2009; published 31 December 2009)

Certain aspects of the recently proposed antisymmetrized α-particle product state wave function, or THSR (Tohsaki-Horiuchi-Schuck-Röpke) α-cluster wave function, for the description of the ground state in ^{8}Be, the Hoyle state in ^{12}C, and analogous states in heavier nuclei are elaborated in detail. For instance, the influence of antisymmetrization in the Hoyle state on the bosonic character of the α particles is studied carefully. It is shown to be weak. Bosonic aspects in Hoyle and similar states in other self-conjugate nuclei are, therefore, predominant. Another issue is the de Broglie wavelength of α particles in the Hoyle state, which is shown to be much larger than the inter-α distance. It is pointed out that the bosonic features of low-density α gas states have measurable consequences, one of which, enhanced multi-α decay properties, has likely already been detected. Consistent with experiment, the width of the proposed analog to the Hoyle state in ^{16}O at the excitation energy of $E_x = 15.1$ MeV is estimated to be very small (34 keV), lending credit to the existence of heavier Hoyle-like states. The intrinsic single-boson density matrix of a self-bound Bose system can, under physically desirable boundary conditions, be defined unambiguously. One eigenvalue then separates out, being close to the number of α particles in the system. Differences between Brink and THSR α-cluster wave functions are worked out. No cluster model of the Brink type can describe the Hoyle state with a single configuration. On the contrary, many superpositions of the Brink type are necessary, implying delocalization toward an α-product state. It is shown that single α-particle orbits in condensates of different nuclei are almost the same. It is thus argued that α-particle (quartet) antisymmetrized product states of the THSR type are a very promising novel and useful concept in nuclear physics.

DOI: 10.1103/PhysRevC.80.064326 PACS number(s): 21.60.Gx

I. INTRODUCTION

Recently, it has been pointed out that certain states in self-conjugate nuclei around the α-particle disintegration threshold can be described as product states of α particles, all in the lowest $0S$ state. Considerable theoretical and experimental activity has developed since this idea was first put forward in 2001 [1]. In this article, we want to further dwell on the basic foundations and predictions of this concept since the usefulness of the latter has recently been questioned [2].

In Refs. [3–5], it was pointed out that in homogeneous nuclear matter, α-particle condensation is a possible nuclear phase. Therefore the previously mentioned α-particle product states in finite nuclei have been proposed to be related to boson condensation of α particles in infinite matter [3–5]. The infinite matter study used a four-particle (quartetting) generalization of the well-known Thouless criterion for the onset of pairing as a function of density and temperature. The particular finding in the four-nucleon case was that α-particle condensation can only occur at very low densities, where the quartets do not overlap appreciably. This is contrary to the pairing case where, in weak coupling situations, the Cooper pairs may also strongly mix. It is interesting to note that the low-density condition for quartetting was, meanwhile, confirmed in Ref. [6], with a theoretical study in cold-atom physics.

Concepts developed for infinite nuclear matter are of value also for interpreting properties in finite nuclei and for constructing useful approximations. As examples, we refer to pairing, two and more body correlations, and one-body occupation numbers. Pairing is believed to occur in neutron stars, which are considered to be infinite neutron matter becoming superfluid below a critical temperature. Pairing is also a useful concept in many finite nuclei, in spite of the fact that nuclei are not macroscopic objects. Therefore, in reality, they are only in a fluctuating state, and we have to project, for example, a BCS state on a definite number of nucleons. In spite of the finiteness of nuclei, the BCS state remains a useful approximation for the quantum state. For example, the strong reduction of measured moments of inertia of such nuclei compared with classical values are explained as a consequence of superfluidity [7].

The α-particle condensed states may also be of relevance in finite nuclei. As already pointed out, in Ref. [1] (see also

 ©2009 The American Physical Society

Ref. [8]), we interpret the Hoyle state, that is, the 0_2^+ state at $E_x = 7.65$ MeV in ^{12}C, as a product state of three α particles and predict that Hoyle-like states very likely also exist in low-density states in heavier $n\alpha$ nuclei, close to the $n\alpha$ disintegration threshold. Examples for ^{16}O and ^{20}Ne have been presented in Refs. [1,9], employing the so-called THSR wave function, proposed by Tohsaki, Horiuchi, Schuck, and Röpke. It is analogous to the (number-projected) BCS wave function, replacing, however, Cooper pairs by α particles (quartets). In addition, we showed that pure product states of α particles in the threshold states are realized to about 70% [10–12]. We thus define a state of condensed $n\alpha$ particles, if, in a nuclear state, the latter forms are in good approximation of a bosonic product state, all bosons occupying the lowest quantum state of the corresponding bosonic mean-field potential.

In this article, we will further investigate the concepts and consequences of the THSR wave function. We will carefully study the effect of antisymmetrization on the bosonic character of the α particles in the Hoyle state. It will be found that, compared to the ground state, its influence is very weak, but not negligible, and, in a sense, is necessary for the α-particle gas state of low density to be formed and stabilized. We also focus on measurable properties that are adequately described in this approximation. Considering special results, we show the usefulness of this novel type of α-cluster wave function.

The article is organized as follows. In Sec. II, we elaborate on the difference between "Brink"- and THSR-type wave functions and demonstrate this first for the most simple case of ^{8}Be. Section III is dedicated to a study of the antisymmetrization effects between the α particles in the Hoyle state, and in Sec. IV, the de Broglie wavelength of α particles in the Hoyle state is studied. In Sec. V, we discuss some measurable consequences of the bosonic character of α particles in compound states, while Sec. VI considers decay properties of Hoyle-like states, and Sec. VII reveals the similarity of α wave functions in Hoyle-like states in nuclei with different numbers of α particles. Finally, in Sec. VIII, we conclude.

II. DELOCALIZED α-PARTICLE CONDENSATE VERSUS LOCALIZED BRINK-TYPE WAVE FUNCTIONS

In Ref. [2], it is claimed that the proposed THSR wave function for the description of loosely bound α-particle states is an approximation to existing nuclear α-cluster states. The authors essentially have in mind localized cluster states of the Brink type [13]. In this section, we will show in detail, presenting new investigations, that the situation is just the contrary: States that have well-born-out $n\alpha$-cluster structures like, for example, the ground- and low-lying states of ^{8}Be and the Hoyle state in ^{12}C are much more adequately described by THSR than by Brink wave functions.

Wave functions for self-conjugate light nuclei that incorporate α-cluster substructures have been in use in nuclear physics for about half a century [14]. Two $n\alpha$ nuclei have been at the forefront of the investigations, ^{8}Be and ^{12}C, with two and three α particles, respectively. The starting point has always been practically the same, that is, for the individual α particles, an intrinsic translationally invariant mean-field wave function of Gaussian type, representing the free space α-particle wave function, is taken, whereas the center of mass (cm) motion is either determined from a full variational principle or limited parametrized ansätze reflecting certain underlying ideas of the α-particle motion have been assumed. Let us, therefore, write for an $n\alpha$ nucleus the typical following α-cluster wave function:

$$\begin{aligned}\Phi_{n\alpha}(\boldsymbol{r}_{1,1},\ldots,\boldsymbol{r}_{n,4}) &= \mathcal{A}[\chi(\boldsymbol{R}_1,\boldsymbol{R}_2,\ldots,\boldsymbol{R}_n) \\ &\quad\times\phi_{\alpha_1}(\boldsymbol{r}_{1,1},\ldots,\boldsymbol{r}_{1,4})\cdots\phi_{\alpha_n}(\boldsymbol{r}_{n,1},\ldots,\boldsymbol{r}_{n,4})], \quad (1)\end{aligned}$$

where $\mathcal{A}$ is the antisymmetrizer, $\boldsymbol{R}_i$ is the cm coordinates of the α particle, and

$$\phi_{\alpha_k}(\boldsymbol{r}_{k,1},\ldots,\boldsymbol{r}_{k,4}) \propto \exp\left[-\sum_{1\leqslant i<j\leqslant 4}(\boldsymbol{r}_{k,i}-\boldsymbol{r}_{k,j})^2/(8b^2)\right], \quad (2)$$

which is the normalized intrinsic wave function of the α particle with a $(0S)^4$ shell-model configuration. With b being a variational parameter, it is well known that Eq. (2) can describe the free α particle quite well. The α-particle wave functions in Eq. (1) are fixed to their free-space form. The wave function χ for the cm motion of the α particles with $\boldsymbol{R}_i = 1/4(\boldsymbol{r}_{i,1}+\boldsymbol{r}_{i,2}+\boldsymbol{r}_{i,3}+\boldsymbol{r}_{i,4})$ is, of course, also chosen translationally invariant; that is, it depends only on the relative coordinates $\boldsymbol{R}_{ij} = \boldsymbol{R}_i - \boldsymbol{R}_j$ or on the corresponding Jacobi coordinates. The spin-isospin part in Eq. (1) is not written out but rather is supposed to be of scalar-isoscalar form. We will not mention it henceforth. As already pointed out, the cm wave function is either determined from a full variational calculation, minimizing the energy, or one adopts a restricted variational ansatz. A famous example is the so-called Brink wave function, which places the α particles at certain positions in space [13]. For example, in the case of ^{8}Be, this is

$$\chi_R^{\text{Brink}}(\boldsymbol{R}_1,\boldsymbol{R}_2) \propto \exp[-(\boldsymbol{R}_1-\boldsymbol{R}/2-(\boldsymbol{R}_2+\boldsymbol{R}/2))^2/b^2], \quad (3)$$

with an obvious generalization to the case of $n\alpha$ particles. Usually, in Eq. (3), b has the same value as for the free-space α particles, and then Eq. (3) implies that the two α particles are placed a relative distance $\boldsymbol{R}$ apart from one another. Though this kind of geometrical, crystallike view of the cluster structure works well for many cases, for instance, parity-violating $^{12}\text{C}+\alpha$, $^{16}\text{O}+\alpha$, and $^{40}\text{Ca}+\alpha$ structures in ^{16}O, ^{20}Ne and ^{44}Ti, respectively [15–17], and also when neutrons are involved [18], it has been, on the contrary, known for several decades that this picture fails for the description of the famous Hoyle state, that is, the 0_2^+ state in ^{12}C.

Since such basic results of cluster physics may not be common knowledge, we here want to present a study with Brink-type cluster wave functions and also compare it with another variational ansatz for χ with the diametrically opposite point of view of completely delocalized α particles, namely, the THSR wave function cited earlier [1]. There, the following

form for χ is adopted:

$$\chi^{\rm THSR}_{n\alpha}(\boldsymbol{R}_1, \boldsymbol{R}_2, \ldots, \boldsymbol{R}_n) = \chi_0(\boldsymbol{\mathcal{R}}_1)\chi_0(\boldsymbol{\mathcal{R}}_2)\cdots\chi_0(\boldsymbol{\mathcal{R}}_n), \quad (4)$$

with $\boldsymbol{\mathcal{R}}_i = \boldsymbol{R}_i - \boldsymbol{X}_G$, where $\boldsymbol{X}_G = (\boldsymbol{R}_1 + \cdots + \boldsymbol{R}_n)/n$ is the total cm coordinate and

$$\chi_0(\boldsymbol{\mathcal{R}}) = \exp[-2(\boldsymbol{\mathcal{R}}^2/B^2)], \quad (5)$$

which is a Gaussian with a large width parameter B of the nucleus's dimension. The product of n identical $0S$ wave functions reflects the boson condensate character, discussed in Sec. I. This feature is realized as long as the action of the antisymmetrizer in Eq. (1) is sufficiently weak. It also is useful to notice that with Eqs. (4) and (1), we can write, for Eq. (1),

$$\Phi_{n\alpha} \to \langle \boldsymbol{r}_{1,1}, \ldots, \boldsymbol{r}_{n,4}|{\rm THSR}\rangle = \mathcal{A}[\psi_{\alpha_1}\psi_{\alpha_2}\cdots\psi_{\alpha_n}], \quad (6)$$

where

$$|{\rm THSR}\rangle = |{\rm THSR}(B)\rangle \equiv \mathcal{A}|B\rangle \quad (7)$$

$$\langle \boldsymbol{r}_{1,1}, \ldots, \boldsymbol{r}_{n,4}|B\rangle = \psi_{\alpha_1}\psi_{\alpha_2}\cdots\psi_{\alpha_n}, \quad (8)$$

where $\psi_{\alpha_i} = \chi_0(\boldsymbol{\mathcal{R}})\phi_{\alpha_i}$ and the definitions of Eqs. (7) and (8) will be useful later. Equations (6)–(8) highlight the analogy of the THSR wave function with the number-projected BCS wave function for pairing

$$\langle \boldsymbol{r}_{1,1}, \ldots, \boldsymbol{r}_{n,2}|{\rm BCS}\rangle = \mathcal{A}[\phi_{\rm pair}(\boldsymbol{r}_{1,1}, \boldsymbol{r}_{1,2}) \cdots \phi_{\rm pair}(\boldsymbol{r}_{n,1}, \boldsymbol{r}_{n,2})], \quad (9)$$

where $\phi_{\rm pair}(\boldsymbol{r}_{i,1}, \boldsymbol{r}_{i,2})$ is the Cooper pair wave function.

This type of condensate wave function has known, in the meantime, considerable success, notably with an accurate description of the Hoyle state, proposing it as the first of a series of excited states in $n\alpha$ nuclei with α-particle product character. Usually, one employs Jacobi coordinates $\boldsymbol{\xi}_i$, and then the THSR ansatz for χ is given by

$$\chi^{\rm THSR}_{n\alpha} = \exp\left(-2\sum_{i=1}^{n-1}\mu_i\frac{\boldsymbol{\xi}_i^2}{b^2 + 2\beta^2}\right), \quad (10)$$

where $\mu_i = i/(i+1)$. A slight generalization of Eq. (10) is possible, taking into account nuclear deformation (see the subsequent discussion).

Before discussing the Hoyle state, we want to study ^{8}Be in some detail because even this nucleus, which is known to have intrinsically a two-α dumbbell structure, can very well be described in the laboratory frame with the delocalized THSR wave function. Let us repeat Eq. (1) for this particular case:

$$\Phi_{2\alpha} = \mathcal{A}[\chi(\boldsymbol{R}_{12})\phi_{\alpha_1}\phi_{\alpha_2}], \quad (11)$$

with $\boldsymbol{R}_{12} = \boldsymbol{R}_1 - \boldsymbol{R}_2$. Note that Eq. (11) is a fully antisymmetric and translationally invariant wave function in $8 - 1 = 7$ coordinates. Minimizing for a given Hamiltonian with N-N forces and Coulomb force [14], the ground-state energy with respect to χ leads straightforwardly to a Schrödinger-type equation for χ, corresponding to the resonating group method (RGM) [19,20]:

$$\langle\phi_{\alpha_1}\phi_{\alpha_2}|\widehat{H} - E|\mathcal{A}[\chi(\boldsymbol{r})\phi_{\alpha_1}\phi_{\alpha_2}]\rangle = 0. \quad (12)$$

With the usual definition of RGM, this equation is transformed into a standard Schrödinger equation for the wave function

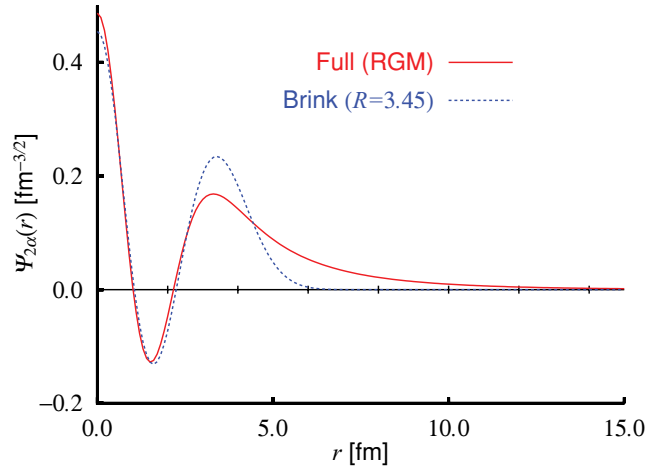

FIG. 1. (Color online) Radial parts of wave functions $\Psi_{2\alpha}(\boldsymbol{r})$ for the full RGM solution (full line) and single Brink component with $R = 3.45$ fm (dotted line). The Volkov force no. 1 is taken with Majorana parameter value $M = 0.56$.

$\Psi_{2\alpha}(\boldsymbol{r})$ of the relative motion of the two α particles:

$$\int d\boldsymbol{r}'\widetilde{h}(\boldsymbol{r}, \boldsymbol{r}')\Psi_{2\alpha}(\boldsymbol{r}') = E\Psi_{2\alpha}(\boldsymbol{r}), \quad (13)$$

$$\Psi_{2\alpha}(\boldsymbol{r}) = \int d\boldsymbol{r}' n^{1/2}(\boldsymbol{r}, \boldsymbol{r}')\chi(\boldsymbol{r}'), \quad (14)$$

$$\widetilde{h}(\boldsymbol{r}, \boldsymbol{r}') = \int d\boldsymbol{r}_1 d\boldsymbol{r}'_1 n^{-1/2}(\boldsymbol{r}, \boldsymbol{r}_1) \times h(\boldsymbol{r}_1, \boldsymbol{r}'_1)n^{-1/2}(\boldsymbol{r}'_1, \boldsymbol{r}'), \quad (15)$$

where

$$n(\boldsymbol{r}, \boldsymbol{r}') = \langle\delta(\boldsymbol{R}_{12} - \boldsymbol{r})\phi_\alpha^2|\mathcal{A}[\delta(\boldsymbol{R}_{12} - \boldsymbol{r}')\phi_\alpha^2]\rangle$$
$$h(\boldsymbol{r}, \boldsymbol{r}') = \langle\delta(\boldsymbol{R}_{12} - \boldsymbol{r})\phi_\alpha^2|\widehat{H}|\mathcal{A}[\delta(\boldsymbol{R}_{12} - \boldsymbol{r}')\phi_\alpha^2]\rangle. \quad (16)$$

In Eq. (16), $\widehat{H}$ is the microscopic Hamiltonian under consideration, and $\phi_{\alpha_1}\phi_{\alpha_2}$ is abbreviated by ϕ_α^2.

As mentioned, Eqs. (12) and (13) have been solved with very high accuracy for the past 50 years, with excellent results for all low-energy properties of ^{8}Be [14]. The radial part of the wave function $\Psi_{2\alpha}(\boldsymbol{r})$ is shown in Fig. 1 by the full line. We see that there exist two nodes, an effect that stems from the Pauli principle. We will now discuss two approximate forms for $\chi(r)$, which are based on the two diametrically opposite views of the nature of ^{8}Be already mentioned: the THSR wave function and the Brink cluster wave function. Let us start with the latter. We have, from Eq. (3),

$$\chi^{\rm Brink}_R(r) = \widehat{P}^{J=0}\exp\left[-\frac{1}{b^2}(\boldsymbol{r} - \boldsymbol{R})^2\right], \quad (17)$$

where $\widehat{P}^{J=0}$ is the projection operator on $J = 0$. In Eq. (17), $\boldsymbol{R}$ is a parameter that allows us to place the two α particles a distance $\boldsymbol{R}$ apart, and $\boldsymbol{r}$ is the relative coordinate between the two α particles, that is, $\boldsymbol{r} = \boldsymbol{R}_1 - \boldsymbol{R}_2$. This ansatz seems reasonable since the microscopic calculation of Ref. [21] indeed indicates that the two α particles are about 4 fm apart. Obviously, the parameter $\boldsymbol{R}$ can be varied to find the optimal position of the α particles. The result of such a

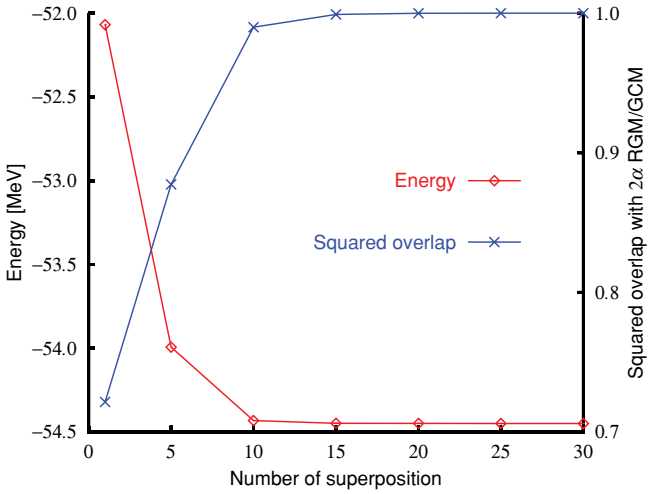

FIG. 2. (Color online) Binding energy given by the wave function $\Phi_{2\alpha}$ and the squared overlap between $\Psi_{2\alpha}$ and $\Phi_{2\alpha}$. For $n = 1$, a single Brink wave function with optimized $R = 3.45$ fm is adopted. See text for definition of $\Phi_{2\alpha}$ and $\Psi_{2\alpha}$. The Volkov force no. 1 is taken with Majorana parameter value $M = 0.56$.

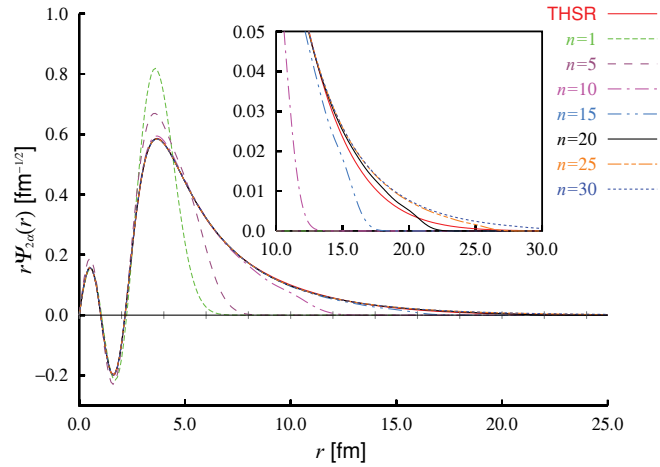

FIG. 3. (Color online) Comparison of THSR wave function with single-component Brink wave function ($n = 1$). The convergence rate with the superposition of several (n) Brink wave functions is also shown (see text for more details).

procedure is shown in Fig. 1, with the dotted line taking the optimal value $R = 3.45$ fm (b is kept fixed at its free-space value, $b = 1.36$ fm). Qualitatively, such a Brink wave function follows the full variational solution (full line). However, in the outer part, for instance, in the exponentially decaying tail, quite strong differences appear. The squared overlap with the exact solution is 0.722. Of course, such Brink wave functions can also serve as a basis, and it is interesting to study the convergence properties. We therefore write, for the ^{8}Be wave function appearing in Eq. (12),

$$\Phi_{2\alpha} = \mathcal{A}[\chi(r)\phi_{\alpha_1}\phi_{\alpha_2}] = \sum_i f_i \Phi^{\mathrm{B}}_{2\alpha}\big(r, R^{(i)}, b\big) \qquad (18)$$

$$\Phi^{\mathrm{B}}_{2\alpha}\big(r, R^{(i)}, b\big) = \mathcal{A}\big[\chi^{\mathrm{Brink}}_{R^{(i)}}(r)\phi_{\alpha_1}\phi_{\alpha_2}\big], \qquad (19)$$

where the $R^{(i)}$ indicates the various positions of the α particles and f_i are the expansion coefficients. The convergence of the squared overlap with the exact solution is studied where we take the positions $R^{(1)} = 1$ fm, $R^{(2)} = 2$ fm, $\ldots$, $R^{(n)} = n$ fm. We start with $n = 5$. In Fig. 2, the convergence rate is shown as a function of n of the squared overlap with the exact solution, and same for the energy. The point of $n = 1$ is with the optimized single Brink wave function [$R^{(1)} = 3.45$ fm]. We see that the convergence is not extremely fast, but for $n = 20$, the squared overlap with the full RGM solution amounts to 0.9999. Also, energy is converged to within 10^{-4}. In Fig. 3, we show the convergence of the wave function $r\Psi_{2\alpha}(r)$. In the inset, we see that there is still a slight change in the far tail going from $n = 25$ to $n = 30$.

Let us now investigate the THSR ansatz for $\chi(r)$. There it is assumed from the beginning that the α particles are delocalized, and a single Gaussian e^{-r^2/B^2} centered at the origin with, however, a large width $B^2 = b^2 + 2\beta^2$, with β being a variational parameter, is taken. Very much improved results over the single-component Brink wave function are obtained. With $\beta = 3.24$ fm, the squared overlap becomes 97.24%. However, practically 100% accuracy, compared with the exact solution, can be achieved starting with a slightly improved ansatz, that is, with an axially symmetric deformed Gaussian, which is then projected on the ground-state spin $J = 0$ (projections on $J = 2, 4$ yield the rotational band of ^{8}Be) [22]:

$$\chi^{\mathrm{THSR}}(r) = \widehat{P}^{J=0} \exp\left(-\frac{r_\perp^2}{b^2 + 2\beta_\perp^2} - \frac{r_z^2}{b^2 + 2\beta_z^2}\right)$$
$$\propto \frac{\exp(-r^2/B_\perp^2)}{ir}\mathrm{Erf}\left(i\frac{(B_z^2 - B_\perp^2)^{1/2}}{B_\perp B_z}r\right), \qquad (20)$$

with $B_i^2 = b^2 + 2\beta_i^2$ and $r_\perp^2 = r_x^2 + r_y^2$, and $\mathrm{Erf}(x)$ is the error function. The second line of Eq. (20) is obtained from a simple calculation.

Such an intrinsically deformed ansatz is, of course, physically motivated by the observation of the rotational spectrum of ^{8}Be, indicating a large value of the corresponding moment of inertia. The minimization of the energy yields $\beta_\perp = \beta_x = \beta_y = 1.78$ fm and $\beta_z = 7.85$ fm. With these numbers, the squared overlap between the exact $\Psi_{2\alpha}$ and $\Psi^{\mathrm{THSR}}_{2\alpha}$ is, with 0.9999, extremely precise.[1] In Fig. 3, we also show that the THSR wave function agrees almost completely, even far out in the tail, with the "exact" solution with 30 Brink components. At the scale of the figure, exact and THSR wave functions cannot be distinguished. Let us also mention that beyond $r \sim 3.5$–4.0 fm, χ^{THSR} and $\Psi_{2\alpha}$ become practically identical in shape, except for a difference of normalization, meaning that approximately from the maximum on, the α particles are no longer influenced by antisymmetrization and behave as pure bosons.

[1]The 2α wave function given in Ref. [22] as the exact 2α RGM solution is different from the one given here. We now realize that to get a better solution, that is, a better energy convergence within 100 eV, we should also include the components of the Brink wave function with values of R as far as 30 fm, whereas previously, Brink components only up to $R = 12.5$ fm have been adopted.

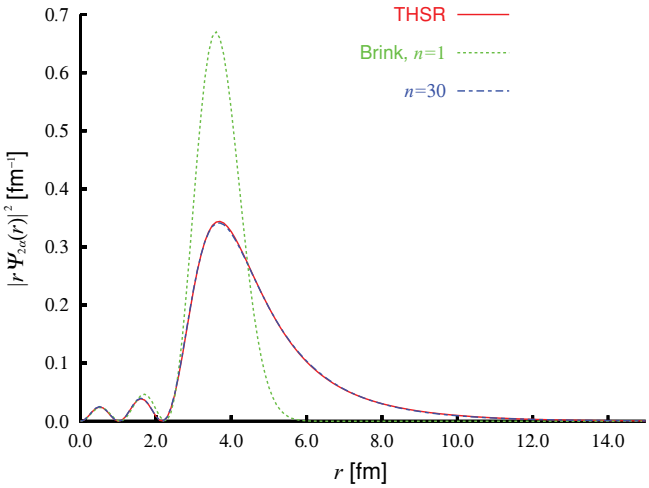

FIG. 4. (Color online) Probability distributions $|r\Psi_{2\alpha}(r)|^2$ for the THSR and single-component Brink (denoted as $n = 1$) wave functions and for the full RGM solution. At the scale of the figure, the two curves of THSR and RGM are indistinguishable. They are normalized as $\int dr|r\Psi_{2\alpha}(r)|^2 = 1$.

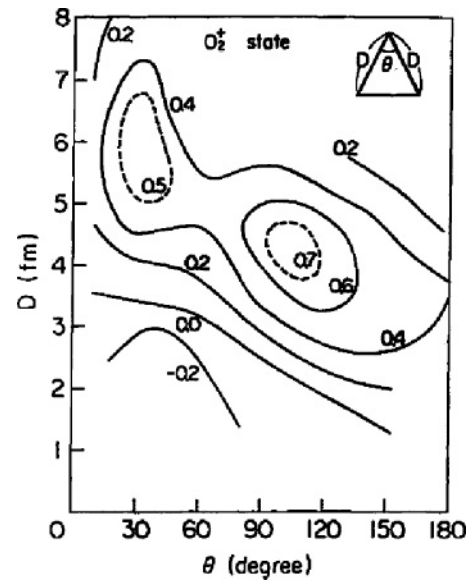

FIG. 5. Structure of the 0_2^+ state in ^{12}C shown by the overlap between the standard Brink cluster wave function of the isosceles configuration and the exact 0_2^+ wave function. Figure is adapted from Ref. [24].

As we saw earlier, the single-component, two-parameter THSR ansatz [Eq. (20)], for the relative wave function of two α particles, seems to grasp the physical situation extremely well. The most important part of this wave function is the outer one beyond some 3 fm. There, the two α particles are in an S wave of essentially Gaussian shape. The corresponding harmonic oscillator frequency is estimated to be $\hbar\omega \sim 2$ MeV. Therefore, as long as the two α particles do not overlap strongly, they swing in a very low frequency harmonic oscillator mode in a wide and delocalized fashion, reminiscent of a weakly bound dimer state. Inside the region $r < 2$–3 fm, where the two α particles heavily overlap, because of the strong action of the Pauli principle, the relative wave function has two nodes and small amplitude, as shown in Fig. 3. Contrary to the outer part of the wave function determined dynamically, the behavior of the relative wave function in this strongly overlapping region is determined kinematically, solely reflecting the r dependence of the norm kernel in Eq. (16). This is clearly seen from the fact that both THSR and Brink wave functions have very nearly the same behavior in this region. It is also instructive to show the probability $|r\Psi_{2\alpha}(r)|^2$, which is presented in Fig. 4. We see that the latter is practically zero for $r < 2$–3 fm, reminiscent of the excluded volume picture that is sometimes adopted when the α particles are treated as pure bosons [23]. Let us repeat: The α particles in ^{8}Be move practically as pure bosons in a relative $0S$ state of very low frequency, as long as they do not get in one another's way, that is, as long as they do not overlap. One should stress that this picture holds after projection on good total momentum and good spin, that is, in the laboratory frame. It is equally true, as already mentioned, that in the intrinsic frame, ^{8}Be can be described as a strongly deformed two-α structure [see ansatz Eq. (20)], reminiscent of a dumbbell.

For the Hoyle state, it has long been known that the situation is qualitatively similar, with, however, a much reduced action of the Pauli principle (see the subsequent discussion). In the work by Uegaki and colleagues [15,24], a contour plot of the overlap between a Brink-type wave function and the full RGM solution for χ of Eq. (1) is shown. We reproduce this as Fig. 5. It is seen that the overlap between the standard cluster wave function and the exact solution is quite poor. In the best case, the squared overlap reaches only about 50%. The authors of that article, which dates three decades back, in view of their finding in Fig. 5, make the following significant statement to characterize the situation: "The 0_2^+ state has a distinct clustering and has no definite spatial configuration. In other words, ^{12}C is dissociated in the 0_2^+ state into weakly interacting three α-clusters, which can be considered as a three boson system." The situation is also highlighted in a recent work by Chernykh *et al.* [25], in which about 55 components of the Brink-type wave functions are needed to reproduce the full RGM solution for the Hoyle state accurately, that is, considerably more than in the case of ^{8}Be.

In what concerns the THSR wave function for the description of the Hoyle state, the situation is slightly more complicated by the fact that the loosely bound three-α configuration is now no longer the ground state, but rather the 0_2^+ state at 7.65 MeV excitation energy. We therefore have to minimize the energy with the THSR wave function

$$\chi_{3\alpha}^{\mathrm{THSR}} = \exp\left[-2\sum_{i=1}^{2}\mu_i\left(\frac{\xi_{i\perp}^2}{b^2+2\beta_\perp^2}+\frac{\xi_{iz}^2}{b^2+2\beta_z^2}\right)\right], \tag{21}$$

where $\boldsymbol{\xi}_{1,2}$ are the two Jacobi coordinates and $\mu_1 = 1/2$, $\mu_2 = 2/3$, under the condition that the 3α wave function $\Phi_{3\alpha}$ is orthogonal to the ground state. $\Phi_{3\alpha}$, to be used for the minimization of the width parameters, can be schematically

written as

$$\Phi^{\rm THSR}_{3\alpha} \propto \widehat{P}^{J=0}\,\widehat{P}^{\rm (g.s.)}_{\perp}\mathcal{A}\Big[\chi^{\rm THSR}_{3\alpha}\phi^3_\alpha\Big], \tag{22}$$

where $\widehat{P}^{\rm (g.s.)}_{\perp}$ keeps Eq. (22) orthogonal to the ground-state configuration, that is, $\widehat{P}^{\rm (g.s.)}_{\perp} = 1 - |0^+_1\rangle\langle 0^+_1|$. The wave function thus obtained has 99.3% squared overlap[2] with the full RGM solution of Fukushima and Kamimura [26]. The corresponding width parameters have the following values: $\beta_\perp = 5.3$ fm and $\beta_z = 1.5$ fm (see Footnote 2). It should be pointed out that the THSR wave function [Eq. (21)] is again of Gaussian type, with a wide extension centered at the origin. It is completely different from a Brink-type wave function, with the three α particles placed at definite values in space. A slight improvement of Eq. (22) can still be achieved in taking the β_i parameters as Hill-Wheeler coordinates and superposing a couple of wave functions of the type of Eq. (22) with different width parameters. Practically 100% squared overlap with the wave function of the full RGM result of Fukushima and Kamimura [26] is then achieved, as documented in Ref. [27]. It should be pointed out that the superposition of several Gaussians of the type of Eq. (21) does not at all change the physical content of the THSR wave function as a wide extended distribution centered around the origin. As we now have three α particles, all in relative S states, one can begin to talk about coherent features, that is, all α particles occupying the same $0S$ orbit. Of course, the Pauli principle is acting, however weakly, and the $0S$ orbit is still occupied to over 70% (see Refs. [10,11,23] and discussion in Sec. VII).

We also would like to attract the attention of the reader to the following important point: In spite of the fact that the THSR wave function describes ^{8}Be very well, it is, of course, clear that no α-particle condensate aspect can be present with only two α particles. This is also borne out by the fact that in ^{8}Be, the α-particle wave function still features quite strongly in the Pauli principle, with the two nodes seen in Fig. 1. On the other hand (see Fig. 14 in Sec. VII), in ^{12}C and ^{16}O, the α-particle wave functions in the condensate states have almost pure $0S$ wave character, and thus the influence of the Pauli principle is much reduced (see Sec. III) and the bosonic condensate feature is borne out. This stems from the fact that, for example, in the Hoyle state, the α particles are, on average, about 70% (see Fig. 5) farther apart than in ^{8}Be, and also that the Hoyle state has to be orthogonal to the ground state of ^{12}C, whereas the α structure in ^{8}Be represents the ground state itself.

Increasing the number of α particles, the full RGM solution is not possible any longer. However, because of the relative simplicity of the THSR ansatz, analogs to the Hoyle state have been found in ^{16}O, ^{20}Ne, always situated close to the $n\alpha$ disintegration threshold [9,12]. Owing to the high agreement with the full RGM results in the ^{8}Be and ^{12}C cases, one can expect that the THSR wave function also gives accurate results for the heavier systems, grasping well the physical situation of loosely bound α particles moving in identical $0S$ orbits. Naturally, the condensate aspect is realized more the larger the number of α particles.

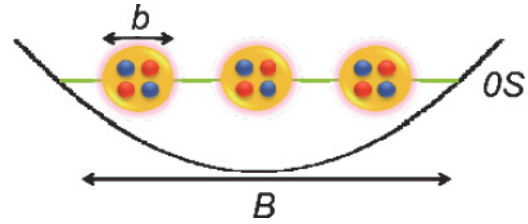

FIG. 6. (Color online) Pictorial representation of the THSR wave function for $n = 3$ (^{12}C). The three α particles are trapped in the $0S$ state of a wide harmonic oscillator (B), and the four nucleons of each α are confined in the $0s$ state of a narrow oscillator (b). All nucleons are antisymmetrized.

Concluding this section, one may simply repeat the well-known knowledge that the weakly bound $n\alpha$-particle states around the $n\alpha$ disintegration threshold are not at all correctly described by standard α-cluster wave functions with a crystal-like structure of the α particles; rather, the condensate aspect is dominant and imposes itself as the correct interpretation. For example, the Hoyle state can be seen as three almost inert α particles moving in their own mean-field potential, to good approximation, given by a wide harmonic oscillator, whereas the α particles are represented by four nucleons captured in narrow harmonic potentials. The situation is given as a cartoon in Fig. 6.

III. INFLUENCE OF ANTISYMMETRIZATION

As already pointed out in the previous sections, a crucial question is whether, for the Hoyle state, the THSR wave function [Eq. (1)] together with Eq. (4) can be considered to good approximation as a product state of α particles condensed with their cm motion into the $0S$ orbital. For this, one has to quantify the influence of the antisymmetrizer $\mathcal{A}$ in Eq. (1). To a certain extent, this question was already answered in earlier works [11]. For instance, in Ref. [11], the single α-particle density matrix $\rho(\boldsymbol{\mathcal{R}}, \boldsymbol{\mathcal{R}}')$ was constructed and diagonalized for the Hoyle state. The result was that the α particles occupied the $0S$ orbit to over 70%. The same result was later obtained with the so-called orthogonality condition model (OCM), which is a very well tested method to describe cluster states [28]. Because of the importance of this result in the present context, we present it again in Fig. 7.

We see that for the ground state, the occupation number distribution agrees with the $SU(3)$ shell model picture (see Ref. [10]), whereas for the Hoyle state, the occupation of the $0S$ cm wave function of the α particle is, as mentioned, over 70%. It is also important to notice that no other state is occupied with more than about 7%, meaning that the occupation of all other states is down by at least a factor of 10. This is a typical scenario for Bose condensed states.

[2]The reason why the present value for the squared overlap is different from 0.97, which was given in Ref. [27], is as follows: In Ref. [27], for the ground-state configuration used in the projection operator $\widehat{P}^{\rm (g.s.)}_{\perp}$, we took the wave function that corresponds to the minimum of the energy surface in Fig. 1 of Ref. [27]. However, in the present definition of $\widehat{P}^{\rm (g.s.)}_{\perp}$, we use the ground-state solution of the Hill-Wheeler equation in the two-parameter space of $\beta_\perp$ and β_z.

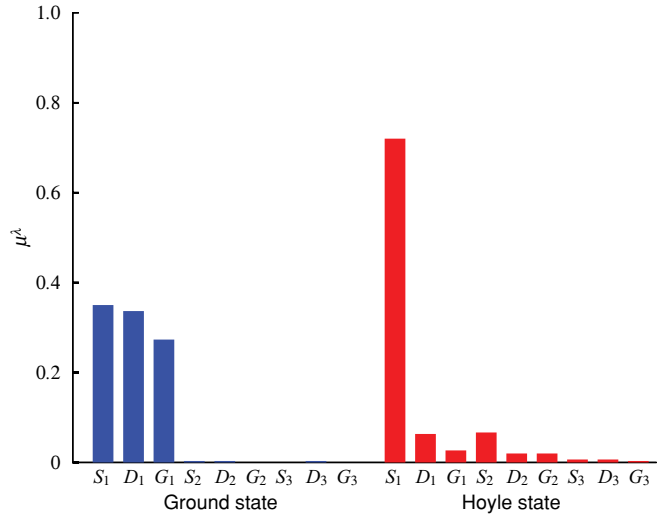

FIG. 7. (Color online) Occupation of the single-α orbitals of the Hoyle state of ^{12}C compared with the ground state [10].

A more direct way to measure the influence of antisymmetrization is to consider the following expectation value of the antisymmetrizer $\mathcal{A}$:

$$N(B) = \frac{\langle B|\mathcal{A}|B\rangle}{\langle B|B\rangle}, \tag{23}$$

where $|B\rangle$ is the THSR wave function [Eq. (6)] without the antisymmetrizer, that is, $|\psi_{\alpha_1}\psi_{\alpha_2}\psi_{\alpha_3}\rangle$ [see Eq. (8)]. The normalization of the antisymmetrizer $\mathcal{A}$ is chosen [29] so that $N(B)$ becomes unity in the limit where the intercluster overlap disappears, that is, for the width parameter $B \to \infty$.

In Fig. 8, we show the expectation value $N(B)$ [Eq. (23)] of $\mathcal{A}$ as a function of the width parameter B. We chose, as optimal values of B for describing the ground and Hoyle states, $B = B_g = 2.5$ fm and $B = B_H = 6.8$ fm, for which the THSR states best approximate the ground state $|0_1^+\rangle$ and the Hoyle state $|0_2^+\rangle$, respectively, which are obtained by solving the Hill-Wheeler equation. In fact, the normalized THSR state, $|\mathrm{THSR}(B)\rangle/\sqrt{\langle\mathrm{THSR}(B)|\mathrm{THSR}(B)\rangle}$, gives the largest squared overlap 0.93 with the ground state $|0_1^+\rangle$ at $B = B_g$. Similarly, it gives the largest squared overlap 0.78 with the Hoyle state $|0_2^+\rangle$ at $B = B_H$.

We should mention that $B_g \neq b$ since the ground state contains α-like correlations that lower the energy with respect to the limit of a pure Slater determinant ($B = b = 1.35$ fm) by roughly 5% [1,27]. We see from Fig. 8 that $N(B_H) \sim 0.62$ and $N(B_g) \sim 0.007$, which indicates that the influence of antisymmetrization is strongly reduced in the Hoyle state compared with the influence in the ground state.

It is worth having a closer look at the behavior of $N(B)$. It is seen that first, this function rises very steeply, whereas for $B > B_H$, the rise is much slower, reflecting the fact that the contribution from the one-nucleon exchange term very slowly fades out [30].

An important point in the present considerations is that the THSR wave function for $B = B_H$ is not automatically orthogonal to the ground state. This is contrary to the situation with condensed cold bosonic atoms, for which the density is

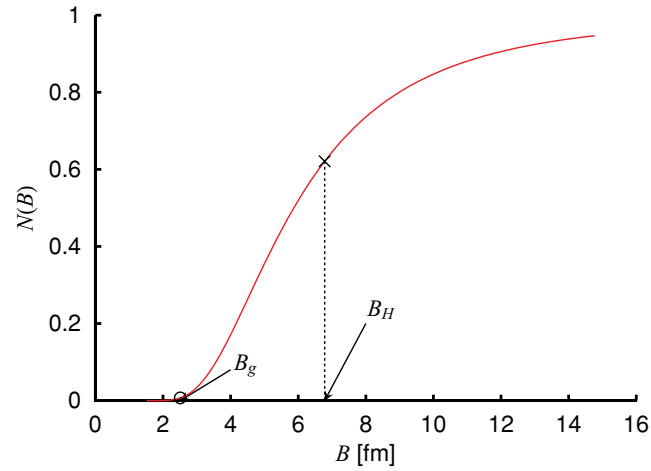

FIG. 8. (Color online) The expectation value of the antisymmetrizer for the product state $|B\rangle$. The values at the optimal B values, B_g for the ground state and B_H for the Hoyle state, are denoted by a circle and a cross, respectively. See the text for the definition of $|B\rangle$, B_g, and B_H.

so low that the overlap of the electron clouds can, on average, be totally neglected. It is nevertheless interesting to calculate the following overlap of $|\mathrm{THSR}\rangle$ with the ground state $|0_1^+\rangle$, obtained by solving the Hill-Wheeler equation, or with $|B_g\rangle$, as a function of B:

$$O(0_1^+, B) = \frac{|\langle 0_1^+|\mathrm{THSR}\rangle|^2}{\langle\mathrm{THSR}|\mathrm{THSR}\rangle}$$

$$O(B_g, B) = \frac{|\langle\mathrm{THSR}(B_g)|\mathrm{THSR}(B)\rangle|^2}{\langle\mathrm{THSR}(B_g)|\mathrm{THSR}(B_g)\rangle\langle\mathrm{THSR}(B)|\mathrm{THSR}(B)\rangle}. \tag{24}$$

From Fig. 9, we find that for both cases, the overlap is less than 0.12, indicating that orthogonality with the ground state is nearly realized.

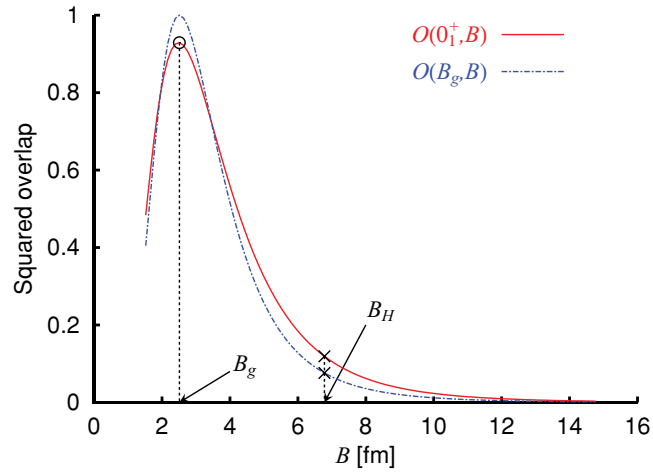

FIG. 9. (Color online) The squared overlap of the state $|B\rangle$ with the ground state and $|B_g\rangle$. The values at the optimal B values, B_g and B_H for the ground and Hoyle states, respectively, are marked by a circle and a cross, respectively. See the text for the definition of $|B\rangle$, $|B_g\rangle$, B_g, and B_H.

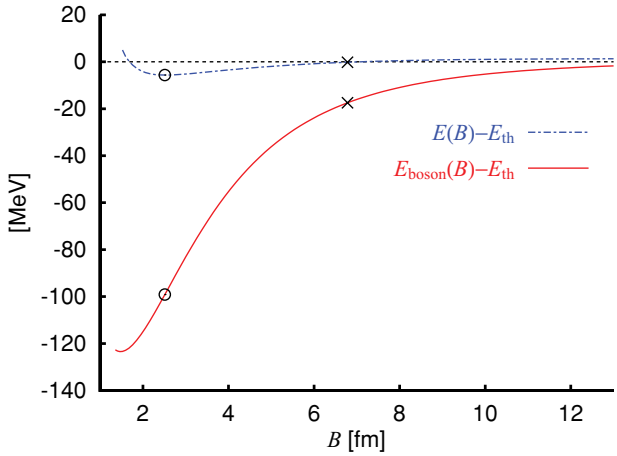

FIG. 10. (Color online) The binding energies for $|\mathrm{THSR}(B)\rangle$ and $|B\rangle$ as a function of B, denoted by $E(B)$ and $E_{\mathrm{boson}}(B)$, respectively. See the text for the definition of $E(B)$ and $E_{\mathrm{boson}}(B)$. They are measured from the calculated 3α threshold energy, $E_{\mathrm{th}} = 3E_\alpha = -82.04$ MeV, where E_α is the binding energy of the intrinsic α particle. Volkov force no. 2 [31] with Majorana parameter $M = 0.59$ and $b = 1.35$ fm are adopted as used in Refs. [26,27]. The values at the optimal B values, B_g and B_H for the ground and Hoyle states, respectively, are marked by a circle and a cross, respectively.

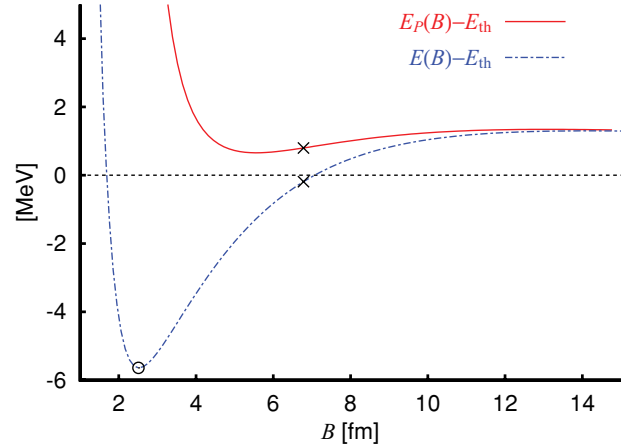

FIG. 11. (Color online) The binding energy in the orthogonal space to the ground state, denoted by $E_P(B)$, together with $E(B)$ in the previous figure. See the text for the definition of $E_P(B)$. They are measured from the calculated 3α threshold energy, $E_{\mathrm{th}} = -82.04$ MeV. Volkov force no. 2 [31] with Majorana parameter $M = 0.59$ and $b = 1.35$ fm are adopted as used in Refs. [26,27]. The values at the optimal B values, B_g and B_H for the ground and Hoyle states, respectively, are marked by a circle and a cross, respectively.

In Fig. 10, the energy curves for the THSR wave function with and without the antisymmetrizer are shown, where

$$E(B) = \frac{\langle \mathrm{THSR}|H|\mathrm{THSR}\rangle}{\langle \mathrm{THSR}|\mathrm{THSR}\rangle} = \frac{\langle B|H\mathcal{A}|B\rangle}{\langle B|\mathcal{A}|B\rangle}$$
$$E_{\mathrm{boson}}(B) = \frac{\langle B|H|B\rangle}{\langle B|B\rangle}. \qquad (25)$$

They are measured from the 3α threshold energy, $E_{\mathrm{th}} = 3E_\alpha = -82.04$ MeV, where E_α is the binding energy of the intrinsic α particle [26,27], obtained with the use of Volkov force no. 2 [31]. The second equality for $E(B)$ in Eq. (25) holds because of the relation $[H, \mathcal{A}] = 0$. The minimum for $E(B)$ is given at $B = B_g$, which corresponds to the ground state. The minimum energy $E(B_g) - E_{\mathrm{th}} = -5.64$ MeV, as also shown in Ref. [27]. On the other hand, $E_{\mathrm{boson}}(B) - E_{\mathrm{th}} \sim -100$ MeV gives unphysically large binding at small B values around B_g, indicating that antisymmetrization plays an important role for the ground state. As B increases, however, the energy drastically gets smaller, and for $B = B_H$, we have $E_{\mathrm{boson}}(B) - E_{\mathrm{th}} = -17.5$ MeV. This means that, compared with the ground state at $B \sim B_g$, the effect of antisymmetrization is much reduced for the Hoyle state. It is, however, still essential to get the energy back on the spot.

It is very important to point out that in this energy curve $E(B)$, the second minimum corresponding to the Hoyle state is not present. This is because the THSR state with $B = B_H$, $|\mathrm{THSR}(B_H)\rangle$, still includes the ground-state components of about 10% what we have seen in Fig. 9. In fact, if we calculate the binding energy

$$E_P(B) = \frac{\langle \widehat{P}_\perp^{(\mathrm{g.s.})}\mathrm{THSR}|H|\widehat{P}_\perp^{(\mathrm{g.s.})}\mathrm{THSR}\rangle}{\langle \widehat{P}_\perp^{(\mathrm{g.s.})}\mathrm{THSR}|\widehat{P}_\perp^{(\mathrm{g.s.})}\mathrm{THSR}\rangle}, \qquad (26)$$

where the explicit orthogonalization to the ground state is taken into account for the THSR state, with $\widehat{P}_\perp^{(\mathrm{g.s.})} = 1 - |0_1^+\rangle\langle 0_1^+|$, like in Eq. (22), there appears the minimum corresponding to the Hoyle state at $B \sim B_H$, as shown in Fig. 11. This is also discussed in Ref. [24], in which Brink-type 3α wave functions are used. We should also mention that the Hoyle state is much better approximated by $|\widehat{P}_\perp^{(\mathrm{g.s.})}\mathrm{THSR}(B)\rangle$ than by $|\mathrm{THSR}(B = B_H)\rangle$, with proper normalization factors for both states. The former state gives the largest squared overlap with the Hoyle state, 0.91 for $B = 6.1$ fm, which should be compared with 0.78 for the latter, a value already mentioned earlier. Thus the small admixture of the ground-state components for the THSR state is never negligible, and the explicit elimination by $\widehat{P}_\perp^{(\mathrm{g.s.})}$ plays an essential role to describe the Hoyle state. It is thus true that the effect of the antisymmetrization is not negligible even for the Hoyle state in a sense that the projection operator $\widehat{P}_\perp^{(\mathrm{g.s.})}$ includes the compact ground-state components, which are strongly subject to the antisymmetrizer. Nevertheless, it is worth emphasizing that as a result of the explicit orthogonalization to the ground state, the Hoyle state cannot have a compact structure but has a dilute density, for which, in the end, the effect of antisymmetrization is small.

Therefore let us point out again that the Hoyle state is to good approximation in a product state of three α particles: About 70% of the α particles are in the $0S$ orbit. Only fewer than 30% of the three α particles are not in the bosonic product state, a fact owing to antisymmetrization. According to Ref. [32], it is expected that in heavier self-conjugate nuclei, the α particles are still farther apart because the stronger Coulomb repulsion lowers the Coulomb barrier. Thus even less influence of antisymmetrization is expected in heavier Hoyle-like states.

IV. DE BROGLIE WAVELENGTH OF α-PARTICLES IN THE HOYLE STATE

In this section, we show, based on results of detailed microscopic calculations, that the de Broglie wavelength λ is larger by almost an order of magnitude than the inter-α-particle distance of about 3–4 fm.

The de Broglie wavelength of the α particles moving in the Hoyle state can be estimated from the resonance energy of ^{8}Be being roughly 100 keV. Otherwise, one can estimate the kinetic energy of the α particles from a bosonic mean-field picture using the Gross-Pitaevskii equation [32]. Figure 3 in Ref. [32] shows the mean-field potential of α particles in the Hoyle state, with an indication of the position of the single α-particle energy (180 keV). The kinetic energy of the single α particle is calculated to be 380 keV. From this, the de Broglie wavelength $\lambda = h/(2M_\alpha E)^{1/2}$ is estimated to be of a lower limit of approximately 20 fm. A more reliable estimate of the de Broglie wavelength is obtained using the expectation value of k^2 for the wave number k of the α particle in the Hoyle state, evaluated from the momentum distribution of the α particle, $\rho(k)$, in Fig. 12, obtained by a 3α OCM calculation [10]. The result is $\lambda = 2\pi/\sqrt{\langle k^2\rangle} \sim 20$ fm, consistent with the previous value. These estimates all indicate that the de Broglie wavelength is much longer than the inter-α-particle distance, favoring a mean-field approach.

All these facts make the Bose aspects of the α particles, in the sense defined in Sec. I, plausible, and they may reveal specific features of coherence, as implied by the notion of a bosonic product state. In the case of nuclear pairing, where the number of bosonic constituents, namely, the Cooper pairs, is finite and not much larger than the number of α particles in light, self-conjugate nuclei, the collective properties of the 0^+ ground states and the coherence of these states have been revealed experimentally very early, the most conspicuous example being the strong reduction of the moment of inertia of superfluid deformed nuclei from its classical value and the strong enhancement of the two-neutron transfer to the ground states [7,33]. The even-odd staggering in the nuclear masses reveals pairing, but not necessarily coherence properties of the pairing state. All these effects of superfluidity are difficult to put into evidence for α-particle condensates for the simple reason that they are resonances around the α disintegration threshold with a finite lifetime. However, instead of pair transfer, one can observe α decay. Similar to two-neutron transfer, because of phase coherence, once a first α particle leaves the nuclear system, the probability that a second, third, and so on will be emitted should be enhanced. This is precisely what we want to report in the following.

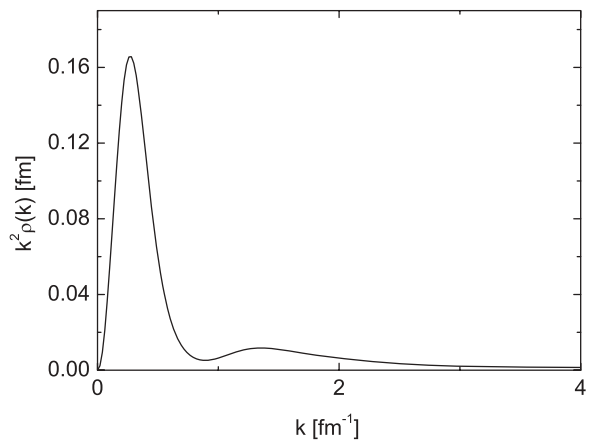

FIG. 12. Momentum distribution of the α particle in the Hoyle state [10].

V. MEASURABLE CONSEQUENCES OF LOOSELY BOUND α-PARTICLE STATES

It is of great importance and interest to discuss eventual measurable consequences for the signature of boson condensates in nuclei. So far, practically all measured quantities of the Hoyle state in ^{12}C have been reproduced with the THSR wave function with rather good accuracy, without any adjustable parameter [27]. For instance, it can be affirmed that the Hoyle state has quite dilute density, about only 1/3–1/4 of the density of the ground state of ^{12}C. The density of the Hoyle state is about the same, or slightly less than, the density of ^{8}Be. To illustrate this dramatic effect, it is sufficient to state that the density at the origin is only half of the density in the ground state of ^{12}C [26]. This fact alone suggests that in the Hoyle state and other similar states in heavier $n\alpha$ nuclei mentioned earlier, there is enough space that nucleons cluster into three α particles. The latter mostly interact via the ^{8}Be resonance.

We will now give new interpretations of older experiments involving multiple α-particle decay out of compound states, which reveal coherence effects of an $n\alpha$-particle gas. The idea is that in excited states of heavier $N = Z$ compound nuclei above a certain excitation energy, a low-density state of α particles can be formed, in a mixed phase of fermions and bosons [34]. Such states can also be formed on top of an inert core like, for example, ^{16}O or ^{40}Ca. The decay process is expected, in light of the present considerations, to show special features, as exemplified later. In particular, the multiple α decay observed does not correspond to results of the Hauser-Feshbach theory of compound nuclear decay.

Previous studies of ^{8}Be emission from excited compound nuclei [35–37] with particle-γ coincidences have shown strong effects in the γ spectra, if statistical α-α emission was compared with ^{8}Be emission. In these experiments, the multiple emission of α particles is registered with the ISIS-ΔE-E particle detection array, in coincidence with the γ decay of the residual nuclei registered with the γ detector array GASP at the Laboratorii Nationale di Legnaro (Italy). As an example, we cite the reaction $^{28}\mathrm{Si} + {}^{24}\mathrm{Mg} \rightarrow {}^{52}\mathrm{Fe}$ at 130 MeV [36], forming a compound nucleus at the excitation energy $E_x = 76$ MeV. For the α-α correlations in these experiments, an enhancement is observed when they are emitted in the same direction. In view of the opening angle (27°) of one individual telescope of the ISIS-ΔE-E system (42 telescopes), we were able to detect the spontaneous decay of the unbound states just at the decay thresholds, namely, of the ^{8}Be and $^{12}\mathrm{C}^*(0_2^+)$ states, into two and three α particles, respectively. The decay energies give relative energies of less

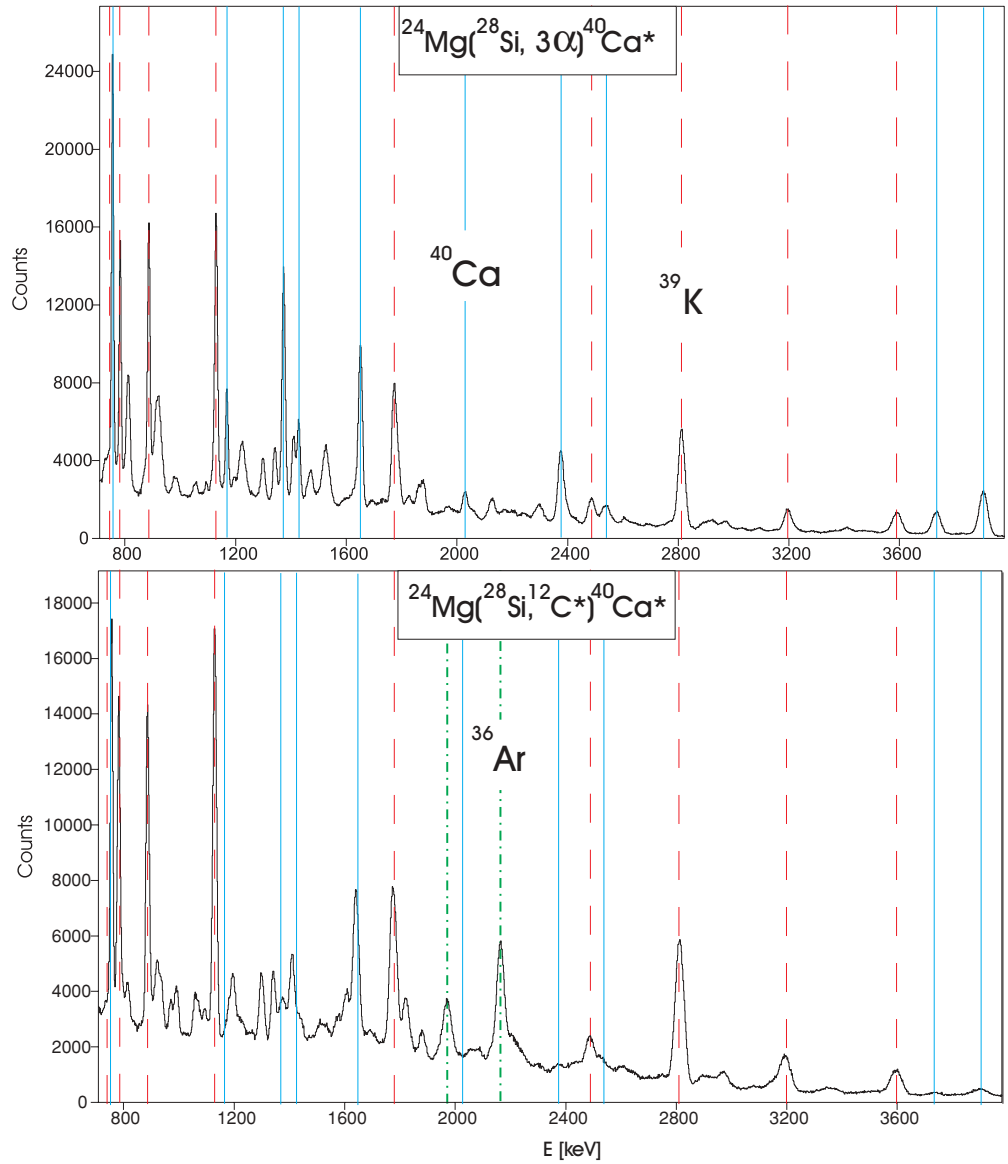

FIG. 13. (Color online) Coincident γ spectra gated with ΔE-E signals with the emission of three random αs in different detectors, in comparison with the spectrum obtained by the $^{12}C^*(0_2^+)$ gate, as indicated in Ref. [36]. The reaction is $^{28}Si + ^{24}Mg$ at 130 MeV. Note the additional ^{36}Ar line in the lower spectrum, which indicates an additional emission of one α. Figure is adapted from Ref. [36].

than 100 keV, and opening angles result, which fit into the solid angle of a single telescope. The corresponding coincident (particle-gated) γ decays are compared with the spectra obtained from statistical α-particle emission into different telescopes, but with the same α multiplicity.

This particularly striking effect is illustrated in Fig. 13 in the case of the previously mentioned reaction $^{28}Si + ^{24}Mg \rightarrow ^{52}Fe \rightarrow ^{40}Ca + 3\alpha$. We compare the $^{12}C^*$ emission (lower spectrum shown in Fig. 13) with that triggered by the statistical decay with three random α particles (here the γ spectra are dominated by transitions in ^{40}Ca and ^{39}K). Quite conspicuous additional γ rays of ^{36}Ar appear in the spectrum gated with $^{12}C^*$ emission, implying that a fourth α particle is emitted, which is not predicted in the Hauser-Feshbach approach for statistical compound decay.

Further explanation of the observed effect within the concept of a gas of almost ideal bosons in ^{52}Fe (in this case, with a ^{40}Ca core) has been proposed in Ref. [38]. If such a compound state is formed in the cited reaction, its characteristic feature is a large radial extension with a very large diffuseness of the density distribution. With the large diffuseness of the potential, the calculation for the emission of the $^{12}C^*$ resonance gives a dramatic lowering of the emission barrier; as compared to the statistical multi-α-particle emission, it amounts to more than 10 MeV. Thus the residual nucleus (^{40}Ca) is populated at much higher excitation energy, and further α decay can occur.

The coherent properties of the threshold states consisting of α particles interacting via their resonances [34] are due to properties of the ^{8}Be ground state or the $^{12}C^*(0_2^+)$ state. As

reported in Sec. IV, the α particles have a large de Broglie wavelength of relative motion of $\lambda = h/(2M_\alpha E)^{1/2} \sim 20$ fm or more. In the decay of the compound nucleus, the decay steps are usually statistically independent, and thus the α particles leave the nucleus one by one. However, for the coherent state, the α particles already exist (large spectroscopic factors), and their wave functions overlap coherently; the decay may be a simultaneous $n\alpha$ decay, keeping the phase relations of their relative motion. In this way, the Coulomb barrier also gets lowered, a fact that further enhances the decay probability. This leads to the observed unbound resonances of ^{8}Be and ^{12}C$^*(0_2^+)$. This result can be interpreted as the observation of bosonic coherence in the compound nucleus.

Such enhanced decays have also been observed in studies of ^{8}Be emission [35,37,39] with the corresponding gated γ spectra. When compared with the statistical decays into two α particles, additional γ transitions are observed. At the time of these experiments, the discussion of α-particle coherence was not considered, and attempts to explain the observed effects within the extended Hauser-Feshbach formalism failed [37].

To summarize, we can state that future dedicated experiments with ΔE-E telescopes, in coincidence with an efficient γ detection array, as described, may be well suited to establishing the existence of THSR-type states in excited $N = Z$ nuclei.

VI. DECAY PROPERTIES

One may ask the question whether Hoyle-like states in nuclei heavier than ^{12}C can exist. An argument can be based on the fact that the α-particle condensate states occur near the α-particle disintegration threshold, which rapidly grows in energy with mass, and thus the level density in which such a condensate state is embedded rises enormously. For example, the α disintegration threshold in ^{12}C is at $E_x = 7.27$ MeV, and in ^{16}O, it is already at $E_x = 14.4$ MeV. Under ordinary circumstances, this could mean that the α-particle THSR state in ^{16}O, which we suppose to be the well-known 0^+ state at $E_x = 15.1$ MeV [12], has a very short lifetime, and in Ref. [2], a Fermi gas estimate is made in this respect. However, on one hand, it is a fact that the supposed ^{16}O "Hoyle" state at $E_x = 15.1$ MeV has experimentally, for such a high excitation energy, a startling small width of 160 keV, and on the other hand, it is easily understandable that such an exotic configuration as four α particles moving almost independently within the common Coulomb barrier has great difficulty for decay into states lower in energy that all have very different configurations. How else could one explain such a small width of a state this high up in energy? It is precisely one of the strong indications of Hoyle-like states that they should be unusually long-lived. It is furthermore well known that the Hoyle state cannot be explained even with the most advanced shell-model calculations. Its energy comes at 2–3 times its experimental value [40]. This is a clear indication that shell-model configurations only couple extremely weakly to α gas states. One can argue that many of the states in ^{16}O below $E_x = 15.1$ MeV are of shell-model type. There are also α-^{12}C configurations, but since ^{12}C also has a shell-model configuration, it is again difficult for the four α condensate states to decay into.

TABLE I. Partial α widths in the 0_6^+ state of ^{16}O decaying into possible channels and the total width. The reduced widths defined in Eq. (28) are also shown. Variable a is the channel radius.

	$^{12}\mathrm{C}(0_1^+)+\alpha$ ($a = 8.0$ fm)	$^{12}\mathrm{C}(2_1^+)+\alpha$ ($a = 7.4$ fm)	$^{12}\mathrm{C}(0_2^+)+\alpha$ ($a = 8.0$ fm)	Total
Γ_L (keV)	26	8	2×10^{-7}	34
$\theta_L^2(a)$	0.006	0.004	0.15	

Let us make a more quantitative estimate of the decay width of the $E_x = 15.1$ MeV state. On the basis of the R-matrix theory [41], the decay width Γ_L can be given by the following formulas:

$$\begin{aligned}\Gamma_L &= 2P_L(a)\gamma_L^2(a),\\ P_L(a) &= \frac{ka}{F_L^2(ka)+G_L^2(ka)},\\ \gamma_L^2(a) &= \theta_L^2(a)\gamma_{\mathrm{W}}^2(a),\\ \gamma_{\mathrm{W}}^2(a) &= \frac{3\hbar^2}{2\mu a^2},\end{aligned} \tag{27}$$

where k, a, and μ are the wave number of the relative motion, the channel radius, and the reduced mass, respectively, and F_L, G_L, and $P_L(a)$ are the regular and irregular Coulomb wave functions and the corresponding penetration factor, respectively. The reduced width of $\theta_L^2(a)$ is related to the wave function $\Psi(0_6^+)$ of the α condensate in ^{16}O obtained as the sixth 0^+ state in Ref. [12], as follows:

$$\begin{aligned}\theta_L^2(a) &= \frac{a^3}{3}\mathcal{Y}_L^2(a)\\ \mathcal{Y}_L(a) &= \left\langle \left[\frac{\delta(r'-a)}{r'^2}Y_L(\hat{\boldsymbol{r}}')\Phi_L(^{12}\mathrm{C})\right]_0 \middle| \Psi(0_6^+)\right\rangle,\end{aligned} \tag{28}$$

where $\Phi_L(^{12}\mathrm{C})$ is the wave function of ^{12}C, given by the 3α OCM calculation [10]. In Table I, we show the partial α-decay widths of the 0_6^+ state Γ_L decaying into the $\alpha + {}^{12}\mathrm{C}(0_1^+)$, $\alpha + {}^{12}\mathrm{C}(2_1^+)$, and $\alpha + {}^{12}\mathrm{C}(0_2^+)$ channels; total α-decay width, which is obtained as a sum of the partial widths; and reduced widths $\theta_L^2(a)$, defined in Eq. (28). Experimental values are all taken as given by the decay energies. Thus the excitation energy of the calculated 0_6^+ state is assumed to be 15.1 MeV, the one with the observed 0_6^+ state.

The obtained very small total α-decay width of 34 keV, in reasonable agreement with the corresponding experimental value of 160 keV, indicates that this state is unusually long-lived. The reason for this fact can be explained in terms of the present analysis as follows: Since this state has a very exotic structure composed of gaslike four-α particles, the overlap between this state and $\alpha + {}^{12}\mathrm{C}(0_1^+)$ or $\alpha + {}^{12}\mathrm{C}(2_1^+)$ wave functions with a certain channel radius becomes very small, as this is, indeed, indicated by small $\theta_L^2(a)$ values, 0.006 and 0.004, respectively, and therefore by small $\gamma_L^2(a)$ values. These largely suppress the decay widths expressed by Eq. (27), in spite of large values of penetration factors caused by large decay energies of 7.9 and 3.5 MeV into the two channels

$\alpha + {}^{12}\mathrm{C}\ (0_1^+)$ and $\alpha + {}^{12}\mathrm{C}\ (2_1^+)$, respectively. On the other hand, the decay into $\alpha + {}^{12}\mathrm{C}\ (0_2^+)$ is also suppressed because of very small penetration caused by very small decay energy of 0.28 MeV into this channel, even though the corresponding reduced width takes a relatively large value $\theta_L^2(a) = 0.15$, which is natural since the 0_2^+ state of ^{12}C has a gaslike three-α-particle structure. It is very likely that the preceding mechanism holds generally for the α-gas states in heavier $n\alpha$ systems, and therefore such states can also be expected to exist in heavier systems as relatively long-lived resonances.

VII. SIMILARITY OF α-PARTICLE WAVE FUNCTIONS IN HOYLE-LIKE STATES

In Fig. 14, we show, side by side, radial parts of the single-α S orbits (for a definition, see Refs. [10,12,42]) of the Hoyle state (^{12}C) and the 0_6^+ state in ^{16}O. We see an almost identical shape. Of course, the extension is slightly different because of the smallness of the system, that is, we are not dealing with a macroscopic condensate, as discussed previously. The nodeless character of the wave function is very pronounced, and only some oscillations with small amplitude are present in ^{12}C, reflecting the weak influence of the Pauli principle between the α particles (see the discussion in Sec. II). On the contrary, because of their much reduced radii, the "α-like" clusters strongly overlap in the ground states of ^{12}C and ^{16}O, producing strong amplitude oscillations, which take care of antisymmetrization between clusters [10,12]. This example demonstrates the bosonic product nature of the Hoyle state and the 0_6^+ state in ^{16}O.

VIII. DISCUSSION, SUMMARY, AND CONCLUSIONS

In this work, we considerably deepened several aspects of the THSR description of low-density α-particle states in self-conjugate nuclei. We show that the THSR wave function that has α-particle condensate structure in analogy with the number-projected BCS wave function for Cooper pairs grasps the physics of loosely bound α-particle states as the ^{8}Be ground state and the Hoyle state in ^{12}C, much better than the usual cluster wave functions of the Brink type, in which a crystal structure is involved, the α particles with free space extension being placed at certain geometrical positions with respect to one another in the nucleus. Indeed, we have shown for the example of ^{8}Be that the superposition of about 30 Brink-type wave functions is needed to describe the ^{8}Be ground state with the same accuracy as the single-component THSR wave function, which practically coincides with the exact solution of the RGM wave function. Similar results are obtained concerning the Hoyle state, in which about 55 components of the Brink type are needed [25].

One entire section is dedicated to the study of effects from antisymmetrization between the α particles in the THSR (Hoyle) state. We studied the expectation value $N(B)$ of the antisymmetrizer as a function of the width parameter B in the THSR wave function, which determines the mean distance between the α particles, and found that $N(B)$ rises very fast as a function of B. For the Hoyle state, with $B = B_H$, $N(B_H)$ is about 0.62, whereas for the ground state, that is, $B = B_g$, we find that $N(B_g)$ is about 0.007. So this value increases from the ground state to the Hoyle state by a factor of about 100, indicating the strongly reduced action of antisymmetrization in the Hoyle state. Similar conclusions are found for energies and orthonormality relations (see Figs. 8–11).

We also discussed the possible experimental consequences of α-particle coherence. This question is more difficult to answer than for nuclear pairing because those states appear only at low density ($\rho = \rho_0/3 \sim \rho_0/4$) and thus correspond to excited states of unusual long lifetimes on nuclear scales ($\sim 10^{-17}$ s for, e.g., the Hoyle state). Transfer experiments of α particles or measurements of moments of inertia, which so clearly demonstrate superfluid features of nuclei in the case of pairing, are therefore very difficult to conceive in the case of α particles. However, instead of transfer, one may investigate decay. For example, in an excited state of ^{52}Fe, if there exists coherence of a certain number of α particles on top of an inert core, the simultaneous decay of two or more α particles will be enhanced with respect to a purely statistical decay. Exactly this feature has been observed and related to α-particle condensation in the reaction $^{28}\mathrm{Si} + {}^{24}\mathrm{Mg}$ at $E_{\mathrm{lab}} = 130$ MeV. However, other experiments may be conceived in the future. For example, with a heavy ion reaction, ^{28}Si may be (Coulomb) excited to the Ikeda threshold of seven-α breakup, that is,

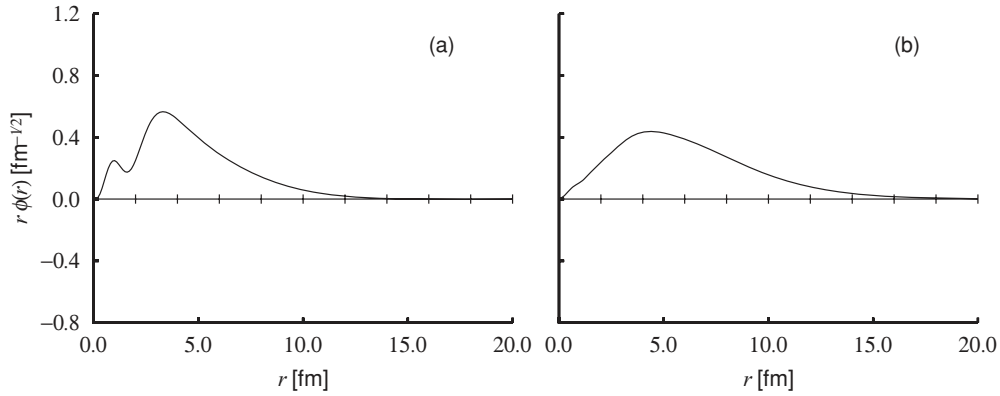

FIG. 14. Radial distributions of the single-α S orbits (a) of the 0_2^+ state in ^{12}C (Hoyle state) and (b) of the 0_6^+ state in ^{16}O.

$E_x = 38.46$ MeV [43], and then seven-α particles may expand as a coherent state verifiable with performant multiparticle detectors [44]. Measuring energies and angles of the α particles may allow us to establish an invariant mass spectrum that identifies THSR states, even if they are relatively broad and hidden among other states, seen via γs or particle evaporation.

Since the α-particle condensate states appear around the $n\alpha$ decay threshold, the higher these states are in the continuum, the heavier the nuclei become. For example, in ^{12}C, the Ikeda threshold for α decay [43] is at $E_x = 7.27$ MeV; in ^{16}O, it is at $E_x = 14.4$ MeV; in ^{24}Mg, it is at $E_x = 28.48$ MeV; and so on. One may object that, because of their high excitation energies, those analogs to the Hoyle state will decay very quickly. However, we argued that these α-gas states have very unusual structure and thus couple only very weakly to states at lower energy. The example of the Hoyle state shows that all states of shell-model structure are practically decoupled. This makes up for the large majority of states. For the supposed analog to the Hoyle state, namely, the 0_6^+ state at $E_x = 15.1$ MeV in ^{16}O, a quantitative estimate of the decay was made, explaining the very small width of 160 keV.

Continuing with this reasoning, it is not at all excluded that α-gas states in even heavier self-conjugate nuclei will have an unusually long lifetime, given their excitation energy high up in the continuum.

Furthermore, the condensate character of the α-gas states has also been pointed out in showing (see Fig. 14) that the condensate wave function of one α particle changes, apart from a trivial size effect, very little in going, for example, from the Hoyle state in ^{12}C to the corresponding state at $E_x = 15.1$ MeV in ^{16}O; that is, a condensate wave function is a $0S$ state.

One of our strong arguments that the α particles in the Hoyle state, and possibly in the 0_6^+ of ^{16}O, form an α-particle gas, captured inside the Coulomb barrier, is deduced from the fact that we constructed a single α-density matrix whose eigenvalues show that the α product states are realized to around 60%–70%, all bosons being in the lowest quantum state [10–12]. The occupancies of all higher quantum levels are down by at least a factor of 10. However, the authors of Ref. [2] mentioned that the way to define the density matrix in a self-bound Bose system with a finite number of particles is not unique and that different definitions might give different occupancies. We followed in this respect the line of thought of Pethick and Pitaevskii in Refs. [45,46], where they say that if in a homogeneous system, there is Bose condensation, then there is no reason that, if the same system is put into an external potential or if the system is self-bound in a mean-field potential, the system may not also be in a nonfragmented condensate state, as long as the intrinsic system is not excited. We showed that our definition of the boson density matrix satisfies this physically very reasonable boundary condition in using Jacobi coordinates for the internal system [42]. We furthermore showed that for the $0S$ harmonic oscillator wave function, the internal one-body density matrix is uniquely determined under another reasonable condition [47]. The uniqueness for more general wave functions is also demonstrated [48,49].

In light of this finding, we would like to discuss again the content of the THSR α-particle condensate wave function [Eq. (6)]. It is very important to remark, as is explained in Ref. [1], that this antisymmetrized α-particle product wave function contains two limits exactly. On one hand, for $B = b$, we have a pure harmonic oscillator wave function because the antisymmetrizer generates out of the product of simple Gaussians all higher nodal wave functions of the harmonic oscillator [50]. On the other hand, for $B \gg b$, the THSR wave function tends to a pure product state of α particles, that is, a mean-field wave function, since in this case, the antisymmetrizer can be neglected. Indeed, B triggers the extension of the nucleus, that is, its average density. For α particles kept at their free-space size (small b), the α particles are then, for large B values, far apart from one another and do not feel any action from the Pauli principle (see a detailed discussion of the action of the antisymmetrizer as a function of density in Ref. [10]). The question is then whether, for example, for the Hoyle state, the preceding wave function is closer to a shell model like a Slater determinant or to an α-particle product state. Precisely this question is answered by the previously discussed eigenvalues of the density matrix. In this respect, it is important to point out that in the calculation of the aforementioned density matrix, always, the total cm motion has been split off in the wave function of Eq. (1), and that for the remaining relative cm coordinates, the Jacobi ones have been used, as is clearly explained in Refs. [10,11]. In Refs. [10,11], it has been shown, as explained, that the α particles in the Hoyle state occupy over 70% of the $0S$ orbit. Therefore the Hoyle state is in good approximation a product of three-α particles, that is, a condensate. This finding is also corroborated by our study on antisymmetrization effects in the Hoyle state in Sec. III. As already mentioned, it has been found that the effects of antisymmetrization are weak.

In summary, we can say that our study clearly shows that the loosely bound α-particle states of very low density, close to the decay threshold in self-conjugate nuclei, are characterized by a shallow self-consistent mean field of wide extension, in which the cm motion of the α particles occupies about 70% of the lowest $0S$ level. In spite of the very different number of particles and other important differences, the situation has, therefore, some analogy with the case of cold atoms. Avoiding vague and qualitative arguments, we hope to have been sufficiently detailed and convincing, based on new insights from precise numerical results, to confirm the existence of low-density bosonic α-particle gas states in nuclei and to affirm the usefulness of this novel concept in nuclear physics described with the THSR wave function.

ACKNOWLEDGMENTS

The authors express special thanks to T. Neff whose detailed studies of the ^{8}Be wave function, made available to us, helped, together with extended discussions, their work appreciably. They also thank Kanto Gakuin University (KGU) and Yukawa Institute for Theoretical Physics at Kyoto University, Japan. Discussions during the KGU Yokohama Autumn School of Nuclear Physics and the YIPQS international molecule workshop held in October 2008 were useful in completing this work.

[1] A. Tohsaki, H. Horiuchi, P. Schuck, and G. Röpke, Phys. Rev. Lett. **87**, 192501 (2001).

[2] N. T. Zinner and A. S. Jensen, Phys. Rev. C **78**, 041306(R) (2008).

[3] G. Röpke, A. Schnell, P. Schuck, and P. Nozières, Phys. Rev. Lett. **80**, 3177 (1998).

[4] M. Beyer, S. A. Sofianes, C. Kuhrts, G. Röpke, and P. Schuck, Phys. Lett. **B448**, 247 (2000).

[5] T. Sogo, R. Lazauskas, G. Röpke, and P. Schuck, Phys. Rev. C **79**, 051301(R) (2009).

[6] B. Doucot, J. Vidal, Phys. Rev. Lett. **88**, 227005 (2002); S. Capponi, G. Roux, P. Lecheminant, P. Azaria, E. Boulat, and S. R. White, Phys. Rev. A **77**, 013624 (2008); P. Lecheminant, E. Boulat, and P. Azaria, Phys. Rev. Lett. **95**, 240402 (2005).

[7] A. Bohr and B. R. Mottelson, *Nuclear Structure* (Benjamin, New York, 1975), Vol. 2; P. Ring and P. Schuck, *The Nuclear Many Body Problem* (Springer, New York, 1980); J.-P. Blaizot and G. Ripka, *Quantum Theory of Finite Systems* (MIT University Press, Cambridge, MA, 1986).

[8] P. Schuck, Y. Funaki, H. Horiuchi, G. Röpke, A. Thosaki, and T. Yamada, Prog. Part. Nucl. Phys. **59**, 285 (2007).

[9] A. Tohsaki, H. Horiuchi, P. Schuck, and G. Röpke, Nucl. Phys. **A738**, 259 (2004).

[10] T. Yamada and P. Schuck, Eur. Phys. J. A **26**, 185 (2005).

[11] H. Matsumura and Y. Suzuki, Nucl. Phys. **A739**, 238 (2004).

[12] Y. Funaki, T. Yamada, H. Horiuchi, G. Röpke, P. Schuck, and A. Tohsaki, Phys. Rev. Lett. **101**, 082502 (2008).

[13] D. M. Brink, in *Proceedings of the International School of Physics "Enrico Fermi," Course 36*, edited by C. Bloch (Academic, New York/London, 1966), p. 247.

[14] R. Tamagaki *et al.*, Prog. Theor. Phys. Suppl. **52**, 1 (1972).

[15] Y. Fujiwara, H. Horiuchi, K. Ikeda, M. Kamimura, K. Katō, Y. Suzuki, and E. Uegaki, Prog. Theor. Phys. Suppl. **68**, 29 (1980).

[16] T. Yamaya, K. Katori, M. Fujiwara, S. Kato, and S. Ohkubo, Prog. Theor. Phys. Suppl. **132**, 73 (1998); F. Michel, S. Ohkubo, and G. Reidemeister, Prog. Theor. Phys. Suppl. **132**, 7 (1998).

[17] T. Wada and H. Horiuchi, Phys. Rev. C **38**, 2063 (1988).

[18] N. Itagaki, T. Otsuka, K. Ikeda, and S. Okabe, Phys. Rev. Lett. **92**, 142501 (2004).

[19] J. A. Wheeler, Phys. Rev. **52**, 1083 (1937); **52**, 1107 (1937).

[20] K. Ikeda, R. Tamagaki, S. Saito, H. Horiuchi, A. Tohsaki-Suzuki, and M. Kamimura, Prog. Theor. Phys. Suppl. **62**, 1 (1977).

[21] R. B. Wiringa, S. C. Pieper, J. Carlson, and V. R. Pandharipande, Phys. Rev. C **62**, 014001 (2000).

[22] Y. Funaki, H. Horiuchi, A. Tohsaki, P. Schuck, and G. Röpke, Prog. Theor. Phys. **108**, 297 (2002).

[23] Y. Funaki, H. Horiuchi, G. Röpke, P. Schuck, A. Tohsaki, and T. Yamada, Phys. Rev. C **77**, 064312 (2008).

[24] E. Uegaki, S. Okabe, Y. Abe, and H. Tanaka, Prog. Theor. Phys. **57**, 1262 (1977); E. Uegaki, Y. Abe, S. Okabe, and H. Tanaka, *ibid.* **59**, 1031 (1978); **62**, 1621 (1979).

[25] M. Chernykh, H. Feldmeier, T. Neff, P. von Neumann-Cosel, and A. Richter, Phys. Rev. Lett. **98**, 032501 (2007).

[26] Y. Fukushima and M. Kamimura, in *Proceedings of the International Conference on Nuclear Structure*, edited by T. Marumori, J. Phys. Soc. Jpn. Suppl. **44**, 225 (1978); M. Kamimura, Nucl. Phys. **A351**, 456 (1981).

[27] Y. Funaki, A. Tohsaki, H. Horiuchi, P. Schuck, and G. Röpke, Phys. Rev. C **67**, 051306(R) (2003).

[28] S. Saito, Prog. Theor. Phys. **40**, 893 (1968); **41**, 705 (1969); Prog. Theor. Phys. Suppl. **62**, 11 (1977).

[29] A. Tohsaki, Y. Funaki, H. Horiuchi, G. Röpke, P. Schuck, and T. Yamada, in *Proceedings of KGU Yokohama Autumn School of Nuclear Physics*, edited by T. Yamada and Y. Funaki, Int. J. Mod. Phys. A **24**, 2003 (2009).

[30] A. Tohsaki-Suzuki, Prog. Theor. Phys. Suppl. **62**, 191 (1977).

[31] A. B. Volkov, Nucl. Phys. **74**, 33 (1965).

[32] T. Yamada and P. Schuck, Phys. Rev. C **69**, 024309 (2004).

[33] W. von Oertzen and A. Vitturi, Rep. Prog. Phys. **64**, 1247 (2001).

[34] W. von Oertzen, Eur. Phys. J. A **29**, 133 (2006).

[35] W. von Oertzen, Phys. Scr. **T88**, 83 (2000).

[36] T. Kokalova *et al.*, Eur. Phys. J. A **23**, 19 (2005).

[37] S. Thummerer, W. von Oertzen, B. Gebauer, S. Lenzi, A. Gadea, D. R. Napoli, C. Beck, and M. Rousseau, J. Phys. G **27**, 1405 (2001).

[38] T. Kokalova, N. Itagaki, W. von Oertzen, and C. Wheldon, Phys. Rev. Lett. **96**, 192502 (2006).

[39] S. Thummerer *et al.*, Phys. Scr. **T88**, 114 (2000).

[40] B. R. Barrett, B. Mihaila, S. C. Pieper, and R. B. Wiringa, Nucl. Phys. News **13**, 17 (2003); B. R. Barrett (private communication).

[41] A. M. Lane and R. G. Thomas, Rev. Mod. Phys. **30**, 257 (1958).

[42] T. Yamada, Y. Funaki, H. Horiuchi, G. Röpke, P. Schuck, and A. Tohsaki, Phys. Rev. A **78**, 035603 (2008).

[43] K. Ikeda, N. Takigawa, and H. Horiuchi, Prog. Theor. Phys. Suppl. **Extra Number**, 464 (1968).

[44] I. Tanihata and W. von Oertzen (private communication).

[45] C. J. Pethick and L. P. Pitaevskii, Phys. Rev. A **62**, 033609 (2000).

[46] L. P. Pitaevskii (private communication).

[47] T. Yamada, Y. Funaki, H. Horiuchi, G. Röpke, P. Schuck, and A. Tohsaki, Phys. Rev. C **79**, 054314 (2009).

[48] Y. Suzuki and M. Takahashi, Phys. Rev. C **65**, 064318 (2002).

[49] Y. Suzuki, W. Horiuchi, M. Orabi, K. Arai, Few Body Syst. **42**, 33 (2008).

[50] T. Yamada, Y. Funaki, H. Horiuchi, K. Ikeda, and A. Tohsaki, Prog. Theor. Phys. **120**, 1139 (2008).